Articles in PresS. Am J Physiol Renal Physiol (August 18, 2010). doi:10.1152/ajprenal.00412.2010

A Single Residue in Transmembrane Domain 11 Defines the Different Affinity for Thiazides between the Mammalian and Flounder NaCl Transporter

by

María Castañeda-Bueno,[1] Norma Vázquez, [1] Ismael Bustos-Jaimes, [2] Damian Hernández, [1] Erika Rodríguez-Lobato, [1] Diana Pacheco-Alvarez, [3] Raquel Cariño-Cortés, [4] Erika Moreno,[4] Norma A. Bobadilla[1], and Gerardo Gamba[1]

[1]*Molecular Physiology Unit,*
Instituto Nacional de Ciencias Médicas y Nutrición Salvador Zubirán,
Instituto Nacional de Cardiología Ignacio Chávez,
and Instituto de Investigaciones Biomédicas, Universidad Nacional Autónoma de México
Tlalpan 14000, Mexico City, Mexico,

[2]*Departamento de Bioquímica, Facultad de Medicina, Universidad Nacional Autónoma de México, Coyoacan, Mexico City Mexico,*

[3]*Escuela de Medicina, Universidad Panamericana, Mexico City, Mexico,*

[4]*Instituto de Ciencias de la Salud, Universidad Autónoma del Estado de Hidalgo. Pachuca, Hidalgo, México*

Running title: Comparative analysis of rat and flounder NCC

Address correspondence to: Gerardo Gamba MD, PhD
Molecular Physiology Unit,
Vasco de Quiroga No. 15,
Tlalpan 14000, Mexico City, Mexico.
Phone: 5255-5513-3868,
Fax 5255-5655-0382,
e-mail: gamba@biomedicas.unam.mx or gerardo.gambaa@quetzal.innsz.mx

Little is known about the residues that control the binding and affinity of thiazide-type diuretics for their protein target, the renal Na^+:Cl^- cotransporter (NCC). Previous studies from our group have shown that affinity for thiazides is higher in rat (rNCC) than in flounder (flNCC) and that the transmembrane region (TM) 8-12 contains the residues that produce this difference. Here, an alignment analysis of TM 8-12 revealed that there are only six non-conservative variations between flNCC and mammalian NCC. Two are located in TM9, three in TM11, and one in TM12. We used site-directed mutagenesis to generate rNCC containing flNCC residues, and thiazide affinity was assessed using *Xenopus laevis* oocytes. Wild-type or mutant NCC activity was measured using $^{22}Na^+$ uptake in the presence of increasing concentrations of metolazone. Mutations in TM11 conferred rNCC an flNCC-like affinity, which was mostly caused by the substitution of a single residue, S575C. Supporting this observation, the substitution C576S conferred to flNCC an rNCC-like affinity. Interestingly, the S575C mutation also rendered rNCC more active. Substitution of S575 in rNCC for other residues, such as alanine, aspartate, and lysine, did not alter metolazone affinity, suggesting that reduced affinity in flNCC is due specifically to the presence of a cysteine. We conclude that the difference in metolazone affinity between rat and flounder NCC is mainly caused by a single residue and that this position in the protein is important for determining its functional properties.

The renal Na^+:Cl^- cotransporter (NCC) is the major transport protein that is expressed in the apical membrane of the distal convoluted tubule, which is located just after the macula densa. The macula densa is where intratubular fluid chloride concentration is sensed to adjust the glomerular filtration rate by the tubuloglomerular feedback mechanism. Thus, salt handling by NCC escapes this regulatory mechanism that affects the urinary salt excretion and thereby the mean circulatory filling pressure (19). Inactivating mutations of NCC in Gitelman's disease or increased activity of NCC due to dysregulation of the cotransporter by the mutant with-no-lysine kinases (WNK1 or WNK4) in Gordon's syndrome lead to arterial blood pressure decreases or increases, respectively, demonstrating the importance of NCC activity in blood pressure regulation (8). This role of NCC has been hypothesized for many years because this cotransporter is the target of the thiazide-type diuretics that were introduced into clinical medicine in 1957 (17). Fifty years later, thiazide diuretics are still recommended by the Joint National Committee for the Prevention**,** Detection**,** Evaluation, and Treatment of High Blood Pressure as the first line pharmacological therapy for patients with arterial hypertension (3). Consequently, thiazides are one of the most frequently prescribed drugs in the world. Little is known, however, about the residues or domains that control the kinetic properties or specificity for thiazide binding to NCC.

NCC is a protein of 1,002 to 1,028 amino acid residues composed of a central hydrophobic domain that contains twelve putative transmembrane-spanning segments (TM 1-12). These segments are interconnected by six extracellular and five intracellular hydrophilic loops. The longer interconnecting segment between TMs 7 and 8 is glycosylated (12) and thus faces the extracellular side. The central hydrophobic domain is flanked by a short amino-terminal domain and a long carboxyl-terminal hydrophilic domain, presumably located within the cell (6) (Figure 1). Tovar-Palacio et al. (21) determined that the critical residues defining the specificity for thiazide inhibition reside within the central hydrophobic domain by studying a chimeric protein.

The chimeric protein contained the transmembrane segments of NCC flanked by the hydrophilic loops of the renal Na^+:K^+:2Cl^- cotransporter NKCC2, which is sensitive to loop diuretics and not to thiazides and behaves in a similar fashion as NCC.

The functional properties of rat and flounder NCCs, such as ion transport kinetics and sensitivity to thiazide-type diuretics, are significantly different; the rat NCC exhibits higher affinity for ions and diuretics (15; 22). These differences were recently exploited in a study in which multiple chimeric proteins between rat and flounder NCCs were produced and analyzed at the functional level (16). In that study, it was observed that the difference in thiazide affinity between cotransporters from different species was conferred by the region containing the TM8 to TM12 segments because a chimeric protein in which this segment from flounder was inserted into the rat NCC exhibited a flounder-like affinity for metolazone and vice versa. Thus, it was proposed that the affinity-defining residues for thiazides are located within the TM8 to TM12 segments of the cotransporter.

The major goal of the present study was to determine the specific amino acid residues within the TM8 to TM12 segments of rat NCC that are responsible for the different affinity for thiazide between the mammalian and flounder orthologues. To do this, we constructed several mutant NCCs and changed key residues within specific TM segments. The functional properties of the resulting proteins were determined by functional expression in *Xenopus laevis* oocytes. Our results show that a single amino acid residue, the serine at position 575 of the rat NCC, corresponding to a cysteine at position 576 in flNCC, explains the difference in thiazide affinity between the mammalian and flounder cotransporters.

METHODS

Xenopus laevis oocyte preparation. Oocytes were harvested surgically from adult female *Xenopus laevis* frogs (Nasco) under 0.17% tricaine anesthesia and incubated in ND96 (in mM: 96 NaCl, 2 KCl, 1.8 $CaCl_2$, 1 MgCl, and 5 HEPES/Tris pH 7.4) in presence of collagenase B (2 mg/ml) for one hour. After four washes in ND96, the oocytes were manually defolliculated and incubated at 18°C in ND96 supplemented with 2.5 mM sodium pyruvate and 5 mg/100 ml of gentamicin overnight. The next day, stage V to VI oocytes (5) were injected with 50 nl of water or 20 ng of cRNA per oocyte. Then, the oocytes were incubated for 2 or 3 days in ND96 with sodium pyruvate and gentamicin, which were changed every 24 hours. Two hours before the uptake experiments were performed, oocytes were incubated in Cl^--free ND96 (96 mM Na^+ isethionate, 2 mM K^+ gluconate, 1.8 mM Ca^{2+} gluconate, 1.0 mM Mg^{2+} gluconate, 5 mM Hepes, 2.5 mM sodium pyruvate, and 5 mg/100 ml gentamicin, pH 7.4) (7).

Site-Directed Mutagenesis. The NCC cDNAs used in this study were the rat and flounder orthologues that we previously isolated from rat kidney (rNCC) (6) and flounder urinary bladder (flNCC) (7). These cDNAs were previously engineered to contain unique silent restriction sites for Sac II and Hpa I at the beginning of TM8 segment and at the end of TM12 segment, respectively (16). Single, double, or triple mutants for TMs 9, 11, and 12 were constructed for these cDNAs using the Quickchange site directed mutagenesis system (Stratagene) following the manufacturer's recommendations. All mutations were confirmed by automatic DNA sequencing from TM8 to TM12 to avoid unwanted mutations elsewhere, and the Sac II to Hpa I fragment from each mutant was subcloned into wild-type NCC by gel purification and ligation of the appropriate cDNA band. All primers used for mutagenesis were custom made (Sigma).

In vitro cRNA translation. cRNA for microinjection was synthesized from wild-type, mutant or chimeric cDNAs previously digested at their 3' end using Not I from New England Biolabs using

the T7 RNA polymerase mMESSAGE mMACHINE^{TM} (Ambion) transcription system. cRNA integrity was confirmed using agarose gels, and the concentration was assessed by absorbance reading at 260 nm (DU 640, Beckman, Fullerton, CA). cRNA was stored frozen in aliquots at -80°C until used.

Transport assays. The activity of the Na^+:Cl^- cotransporter was determined by assessing $^{22}Na^+$ tracer uptake (New England Nuclear) in groups of 10 to 15 oocytes following our protocol (15). Briefly, a 30-min incubation in a Cl^--free ND96 medium containing 1 mM ouabain, 0.1 mM amiloride, and 0.1 mM bumetanide was followed by a 60-min uptake period in a K^+-free, NaCl medium (40 mM NaCl, 56 mM Na-gluconate, 4.0 mM $CaCl_2$, 1.0 mM $MgCl_2$, and 5.0 mM Hepes/Tris, pH 7.4) containing ouabain, amiloride, bumetanide and 2 μCi of $^{22}Na^+$ per ml. Because *Xenopus laevis* oocytes do not express a thiazide-sensitive Na^+:Cl^- cotransporter (7; 15), only one group of water-injected oocytes was included in every experiment to determine the basal, nonspecific trace $^{22}Na^+$ uptake. The affinity for thiazide diuretics was assessed by exposing groups of cRNA-injected oocytes to increasing concentrations of drug (from 10^{-9} to 10^{-4} M). The desired concentration of the diuretic was present in both the incubation and uptake periods. All metolazone-dependency curves were assessed at least twice for each clone. Ion transport kinetics were determined by performing experiments with varying concentrations of Na^+ and Cl^-. Isethionate was used as a Cl^- substitute and NMDG as a Na^+ substitute to preserve osmolarity and ionic strength.

All uptake experiments were performed at 32°C. At the end of the uptake period, oocytes were washed five times in ice-cold uptake solution without isotope to remove tracer in the extracellular fluid. After oocytes were dissolved in 10% sodium dodecyl sulfate, the tracer activity was determined for each oocyte by β-scintillation counting.

Western Blotting. Western blot analysis was used to assess the amount of protein expression in wild-type or mutant-NCC-injected oocytes. Expression of NCC was determined as FLAG-NCC because our cDNA contains a FLAG epitope after the first methionine (16). Proteins extracted from 50 oocytes injected with wild-type or mutant NCCs were quantified by Bradford's technique, and 50 μg of each protein was run per lane using sample buffer containing 6% SDS, 15% glycerol, 0.3% bromophenol blue, 150 mM Tris pH 7.6, and β-mercaptoethanol (when indicated), resolved by Laemmli SDS-polyacrylamide (7.5%) gel electrophoresis, and transferred to a polyvinylidene difluoride (PVDF) membrane. Immunoblotting was performed using anti-FLAG monoclonal antibody (Sigma). Membranes were exposed to anti-FLAG antibody overnight at 4°C, washed and incubated for 60 min at room temperature with alkaline phosphatase-conjugated secondary (anti-mouse) antibody (BIO-RAD) diluted 1:2000 in blocking buffer and washed again. Bands were detected by using Immun-Star Chemiluminescent Protein Detection Systems (BIO-RAD).

Data analysis. All results presented are based on a minimum of three different experiments with at least 12 oocytes per group in each experiment. Results are presented as means of uptake values within groups ± SEM unless otherwise stated. Prism 5.0 was used to fit the kinetic data. Chloride and sodium Km values were determined by fitting the uptake data with the Michaelis-Menten equation. For thiazide, non-linear fittings were done using the Hill equation, from which the IC_{50} values shown in the text were obtained. In all cases, a Hill coefficient close to unity was observed.

RESULTS

Single amino acid residue differences between mammalian and flounder NCC. We have previously shown that the difference in thiazide affinity between rat and flounder NCC is encoded within the TM segments 8 to 12 (16). In addition, we have also observed that thiazide affinity is similar between rat and mouse NCCs (18). Thus, we reasoned that the difference in thiazide affinity between mammalian and flounder NCCs could be due to residue differences between them. We performed an alignment analysis of NCC TMs 8 to 12 using all the available NCC sequences to find the residues that are identical in mammalian orthologues but different in the flounder with a change between mammalian and flounder that is not conservative. As shown in Figure 1, we found only six amino acid residues with these characteristics. The two located in TM segment 9 are the alanine residues 510 and 516, which correspond to threonine and cysteine, respectively, in flounder. The three located in TM segment 11 are alanine, isoleucine, and serine at positions 568, 574, and 575, which correspond to serine, cysteine, and cysteine, respectively, in the flounder NCC. Finally, a valine at position 601 in the rat NCC TM12 is substituted by a threonine in the flounder NCC. No such differences were found in TM8 or TM10, which are almost identical between the mammalian and flounder NCCs. Thus, by site-directed mutagenesis, we introduced the single-point mutations to change one TM segment at a time from rNCC to flNCC. Three mutant clones were generated: mutant TM9 (A510T and A516C), mutant TM11 (A568S, I574C, and S575C), and mutant TM 12 (V601T). As shown in Figure 2, all three mutant cotransporters were functional, as they exhibited a thiazide-sensitive $^{22}Na^{+}$ uptake that was similar to that observed for rNCC. Of note, functional expression observed in the TM11 mutant was significantly higher than in oocytes injected with any of the other clones.

The difference in thiazide affinity between rat and flounder NCC resides in TM11. Rat and flounder NCCs exhibit a difference in thiazide affinity of approximately one order of magnitude

198 (15; 16; 22). Thus, in the present study, we assessed the thiazide dose-response curves in oocytes
199 injected with wild-type rNCC or flNCC cRNA as well as oocytes injected with mutants NCC
200 cRNAs at TM9, TM11, or TM12. The thiazide affinity for all clones was assessed in the same
201 experiment to assure that the oocytes, solutions and metolazone concentration were identical
202 among groups. Figure 3 shows the compilation of five different experiments. As previously
203 shown (16), rat NCC (in blue) and flounder NCC (in red) display a significant difference in
204 affinity for metolazone, which is of about one order of magnitude. Interestingly, the dose-
205 response curves for the rNCC-TM9 mutant (orange) and for the rNCC-TM12 mutant (pink) were
206 similar to that of rNCC. In contrast, the affinity for metolazone in oocytes injected with the
207 rNCC-TM11 mutant cRNA (green) was identical to that observed in oocytes injected with flNCC
208 cRNA. These observations strongly suggested that the difference in metolazone affinity between
209 rat and flounder NCCs is encoded in TM11 and that one to three amino acid residues could be
210 responsible.

211 Rat and flounder NCCs also exhibit a significant difference in affinity for Na^+ and Cl^-
212 ions. Our recent observations suggested that the difference in chloride affinity is encoded within
213 TM segments 1 to 7, while no specific domain seems to be responsible for the difference in
214 sodium affinity (15; 16; 22). We thus analyzed the effect of TM9, TM11, and TM12 mutations
215 for affinity to cotransported ions. The results are shown in Table 1. As expected, the sodium and
216 chloride transport kinetics of all three mutants are similar to each other and to that observed for
217 wild-type rNCC, indicating that these residues play no role in defining transport ion kinetics.

218 ***A serine to cysteine change in TM11 is responsible for the difference in thiazide affinity***
219 ***between rat and flounder NCC.*** Because thiazide affinity between wild-type rNCC and rNCC-
220 TM9 or rNCC-TM12 mutants was similar, no additional analysis was done for these clones. In
221 contrast, rat NCC harboring three mutations in TM11, which correspond to the flounder NCC

sequence, exhibited an affinity for metolazone that was identical to that in flNCC. We therefore further explored the role of each of these amino acid residues. Two of these mutations in TM11 switched the original amino acid for a cysteine residue (I574C and S575C). Cysteines are special residues because they can establish strong covalent interactions that can affect the structural and functional properties of proteins; therefore, we decided to study these two residues first. We used site-directed mutagenesis to create a double mutant rNCC that harbors both the I574C and S575C mutations. In addition, we made two rNCC single mutants containing either the I574C or S575C mutation alone. The effect of these mutations on metolazone affinity was determined. Figure 4 depicts the mean of the IC_{50} values obtained from five different dose-response curves that were assessed simultaneously in oocytes injected with rNCC-TM11, the double mutant I574C S575C, or the single mutants I574C or S575C. Similar to the dose-response curves shown in Figure 3, rNCC-TM11 shifted the metolazone affinity to the right by about one order of magnitude ($p<0.05$ vs. rNCC). A similar shift was observed in oocytes injected with double mutant or the single mutant S575C. In contrast, the I574C mutation had no effect on thiazide affinity because the IC_{50} in oocytes injected with this mutant cRNA was identical to that shown for wild-type rNCC.

If the serine vs. cysteine substitution at position 575 in rat NCC or 576 in flounder NCC is responsible for the difference in affinity for metolazone between species, one would expect that this mutation should be enough to switch the affinity for metolazone in flounder to an IC_{50} similar to that observed in wild-type rat NCC. We thus introduced by site-directed mutagenesis the C576S mutation into flNCC cDNA. Metolazone dose-response curves were performed in three different experiments. A representative experiment is shown in Figure 5A and the mean IC_{50} values from three different experiments are shown in Figure 5B. As expected, the affinity for metolazone was significantly increased by the C576S substitution in flNCC.

We have previously observed that while rat and flounder NCCs exhibit a difference in affinity for thiazide-type diuretics, the profile of inhibition among different thiazides is similar (15; 22). The observed inhibition is greatest for polythiazide, followed by metolazone, bendroflumethiazide, trichloromethaizide, hydrochlorothiazide, and chlorthalidone. This inhibitory profile is similar to thiazide potencies in clinical medicine, as well as their potency to block the [^{3}H]-metolazone binding to renal cortical membranes (1). We assessed the thiazide inhibitory profile of mutant S575C. For all thiazides tested, the IC_{50} in S575C was shifted to the right when compared to rNCC (data not shown). In addition, the inhibitory profile observed was similar to that previously seen for rNCC (15) or to that observed in simultaneous experiments. Thus, substitution of serine 575 to cysteine in rNCC similarly affected the affinity for all thiazide type diuretics tested.

The serine to cysteine substitution affects the NCC basal activity. In the experiments described above, we noticed that functional expression of the rNCC-TM11 mutant was always higher than wild-type NCC by at least 20%. Thus, we assessed the $^{22}Na^+$ uptake in oocytes injected with the same amount of cRNA for wild-type NCC, rNCC-TM11 mutant, or single mutants I574C and S575C rNCC, as determined by densitometry of the cRNA bands in agarose gels. A representative experiment is shown in Figure 6A. The $^{22}Na^+$ uptake in oocytes injected with the rNCC-TM11 mutant or S575C mutant rNCC cRNA was significantly higher than that observed in wild-type rNCC. In contrast, the activity of the I574C cotransporter was similar to wild-type rNCC. Proteins from the same oocytes used in the experiment shown in Figure 6A were extracted and used for western blot analysis. The results of this experiment and the corresponding densitometric analysis are shown in Figure 6B and 6C. No increase in protein expression of TM11 or S575C was observed that would explain the higher $^{22}Na^+$ uptake in these mutants. Together, these observations suggest that the difference in basal activity between the rNCC-

TM11 or S575C mutants and wild-type NCC cannot be explained by changes in protein expression. Therefore, S575C increases the tonic activity of the cotransporter by either improving its surface expression or its translocation rate. Testing these possibilities is beyond the scope of this study.

The decrease of thiazide affinity in rNCC is specific for a cysteine substitution. We have shown that substituting serine for cysteine in rNCC or cysteine for serine in flNCC switched the cotransporter affinity from rat to flounder-like and vice versa. We wanted to know if the decreased thiazide affinity in rNCC-S575C is specifically due to the introduction of the cysteine and, thus, probably related to its capacity to establish disulfide bonds. Another possibility is that this phenomenon could be due to a change in the local environment of this residue produced by the different physical and chemical properties of serine and cysteine. Sulfur and oxygen atoms have different electronegativities, so the polarity of these chemical groups is not identical, with hydroxyls having a higher electronegativity. This produces a weak H-bonding propensity in the sulfhydryl groups of cysteines. In addition, the proton in the sulfhydryl groups of cysteines is much more acidic (pKa 8.18) than the hydroxylic proton of serine. All these different properties could explain the difference in affinity, if, for example, a hydrogen bond established with the thiazide or another residue in the protein is stronger in the presence of a serine. With this in mind, we constructed three more mutants in which serine 575 of rNCC was substituted for a positive, a negative or a neutral amino acid residue, namely lysine, aspartate or alanine, respectively. We reasoned that positive and negative charges could establish an electrostatic interaction that would resemble a hydrogen bond formed by the cysteine/serine, and that the alanine would prevent the formation of any interaction. However, none of the introduced residues would favor the formation of disulfide bonds. As shown in Figure 7A, substitution of serine for lysine resulted in a non-functional cotransporter. In contrast, substitution of serine 575 with alanine or aspartate

293 produced rNCC mutants that exhibited enough $^{22}Na^{+}$ uptake to determine a dose-response curve
294 for metolazone. As shown in Figure 7B, affinity for metolazone was similar in oocytes injected
295 with wild-type rNCC, rNCC-S575A and rNCC-S575D but different from that observed in rNCC-
296 S575C. These observations suggest that it is specifically a change for cysteine in position 575
297 that makes rNCC less sensitive to metolazone.

298 It has been suggested that NCC functions as a homodimer, but it is not clear if the
299 interaction between monomers involves the formation of disulfide bonds (4). If this type of bond
300 is not present between NCC homodimers, then a cysteine difference between rat and flounder
301 NCC could be allowing the flounder cotransporter to form a disulfide bond between monomers
302 that is not present in the mammalian cotransporter. To determine if disulfide bonds are present in
303 NCC dimers and to find out if this is affected by S575C substitution in rNCC, we performed a
304 western blot analysis of proteins extracted from *Xenopus laevis* oocytes microinjected with water,
305 wild-type rNCC, or S575C-rNCC cRNA. Protein extracts were prepared for standard SDS-PAGE
306 with Laemmli buffer with or without reducing agent (5% β-mercaptoethanol). As shown in
307 Figure 8, in the absence of reducing agent, bands of expected size for NCC dimers and monomers
308 are observed in both wild-type NCC and S575C-NCC. When a reducing agent was used, single
309 bands of the expected size for the NCC monomer were present while the bands corresponding to
310 the dimer size were absent. This finding suggests that disulfide bonds are involved in NCC
311 dimerization. No difference, however, was observed between wild-type rNCC and the S575C
312 NCC mutant. As shown in Figure 8, to rule out the possibility that mutant rNCC becomes slightly
313 resistant to the reducing agent due to the presence of an extra disulfide bond, we repeated the
314 experiment using β-mercaptoethanol at different concentrations. No difference between wild-type
315 and mutant NCC was observed at any point.

316

DISCUSSION

In the present study, we show that substituting serine 575 in rat NCC for the cysteine present in flounder NCC at the same position is sufficient to render rat NCC more resistant to thiazides, exhibiting a flounder-like affinity. Supporting these observations, substituting the cysteine 576 in the flounder NCC for the corresponding serine in the rat NCC increased the affinity of flNCC to a mammalian-like IC_{50}. Therefore, a single residue difference in TM11 segment between rat and flounder NCC explains the difference in affinity for thiazides between species. In addition, we observed that substituting the serine 575 in rNCC with other residues than cysteine, such as alanine or aspartate, had no effect upon affinity for thiazides, suggesting that it is not the presence of the serine in this position that increases affinity, but instead it is the absence of a cysteine residue that is present in flNCC. Although it is unknown if loop diuretics or thiazides bind to a similar region in NKCCs and NCC, our observations are supported by previous work on chimeric proteins between shark and human NKCC1 that suggests roles for transmembrane segments 11 and 12 (13).

Two different possible mechanisms can potentially explain the decrease in affinity for metolazone observed in the NCC-S575C mutant. The first mechanism is that this residue may be part of the thiazide binding site on the cotransporter, and the second mechanism is that substitution of S575C may modify the tridimensional configuration of the protein, indirectly affecting the interaction of thiazides with their binding site or the protein's response upon drug binding. Our results favor the second possibility because if serine 575 were part of the thiazide-binding site, it would be expected that substituting the serine with different amino acid residues would result in altered affinity for thiazide. However, our data show (Figure 7) that changes in affinity occur only when serine is substituted with cysteine, suggesting that it is a unique property of cysteines that decreases the thiazide affinity in mutant rNCC-S575C.

Cysteines are very important residues in the tridimensional structure of proteins because they form disulfide bonds. Two types of interactions can be established by the sulfhydryl group in their side chain: hydrogen bonds and disulfide bonds (10). In NCC, the establishment of a hydrogen bond by this cysteine probably would not generate a significant difference in terms of structure, as compared to the structure of the wild-type cotransporter, because the serine originally present in rNCC also possesses the ability to form hydrogen bonds. Thus, a plausible possibility is that the substitution of serine 575 for cysteine may introduce a new covalent bond, changing the tertiary structure of NCC. This substitution could reduce the access of thiazides to their binding site located elsewhere, could introduce a structural change that allosterically affects the binding site for the inhibitor, or could affect the protein's response upon drug binding. According to the hydropathy predictions (6), serine 575 lies approximately in the middle of TM11 segment. A model for the putative configuration of the α-helix formed by TM11 predicts that serine 575 is located in a hydrophilic face of the helix (Supplemental Figure 1), implying that this face could be involved in contacts with other protein domains and not facing the membrane, thus making it possible that changing the serine for cysteine creates the possibility of a disulfide bond formation with another residue in a membrane domain of the same polypeptide or of another NCC monomer. There is evidence that NCC forms homodimers that may be the functional form of the cotransporter; however, the TM segments involved in establishing the interface between monomers are unknown. Although no crystal structure of any member of the SLC12 family is available, the crystal structures of transporters of the APC (amino acids, polyamine, organocation) transporter superfamily, in which the SLC12 family is included, have been reported (20) (9). Two of these transporters, as detailed in the legend of Supplemental Figure 1, present a generally similar folding pattern, with segments 1-10 forming the core

structure of the cotransporter that comprises the ion translocation pathway, and TM 11 and 12 lying outside as accessory segments. This general folding pattern is not only conserved in APC transporters, but is also present in a more distantly related bacterial leucine cotransporter, LeuT (2)(11)(23).Thus, expecting similarities, at least at a general level of structure, between NCC and these transporters is sound. This finding is supported by a recent thorough analysis of the structural conservation among sodium transporters (14). Continuing this line of reasoning, the residue that was found to alter NCC affinity for thiazides would be located in an accessory TM segment. However, it is not possible to speculate on its exact position within this segment. AdiC, one of the crystallized APC transporters, has a dimeric structure in which TM segments 11 and 12 lie outside the core structure and form the interface between the dimers. LeuT also forms dimers, and there is evidence that in the eukaryotic homologues of this cotransporter, TM11 participates in dimerization. Therefore, the cysteine in position 576 of flNCC, could be forming an interaction either with another residue within the same polypeptide chain or located in the second monomer of the NCC homodimer.

Considering the possibility that substituting a serine for cysteine at position 575 in rNCC could be mediating an interaction between NCC monomers, we performed a western blot analysis of wild-type and mutant rNCC-S575C in the absence or presence of reducing agent. The existence of NCC homodimers has been demonstrated previously (4), but that disulfide bonds are involved in the interaction between NCC monomers has never been explored. Thus, we reasoned that the new cysteine introduced could perhaps be creating a new covalent bond between subunits that was originally nonexistent. If this were the case, and if there are no disulfide bonds between wild-type rat NCC monomers, we would expect to see bands corresponding to the homodimers in the absence of reducing agent only in the mutant protein. The result shown in Figure 8, however, suggests that wild-type rNCC forms homodimers in which disulfide bonds are involved, and no

388 difference is observed between the wild-type and mutant NCCs. Also, no difference in resistance
389 to the effects of the reducing agent was observed between the wild-type and the mutant clones
390 when different concentrations of β-mercaptoethanol were used. This finding suggests that no
391 additional intermolecular bonds are formed when serine 575 is switched for a cysteine. However,
392 this observation does not rule out the possibility that this cysteine may be forming a new disulfide
393 bond, perhaps altering the original pattern of disulfide bonds formed between NCC subunits.
394 In summary, we propose that the difference in thiazide affinity observed between
395 mammalian and flounder NCCs is mainly due to a single amino acid residue difference between
396 cotransporters. This residue is located within the transmembrane segment 11. Further
397 investigation will be required to define the mechanism by which substitution of a cysteine in
398 flNCC for a serine in rNCC increases the affinity for thiazides.
399
400

AKNOWLEDGMENT

We are grateful to all members of the Molecular Physiology Unit for suggestions and stimulating discussion.

GRANTS

This work was supported by NIH grant DK-64635 to GG and CONACYT grants 59992 to GG and 104451 to EM.

DISCLOSURES

|No conflicts of interest are declared by the authors.

Reference List

1. **Beaumont K, Vaughn D A and Fanestil D D**. Thiazide diuretic receptors in rat kidney: Identification with [^{3}H]metolazone. *Proc Natl Acad Sci USA* 85: 2311-2314, 1988.
2. **Chen NH, Reith ME and Quick MW**. Synaptic uptake and beyond: the sodium- and chloride-dependent neurotransmitter transporter family SLC6. *Pflugers Arch* 447: 519-531, 2004.
3. **Chobanian AV, Bakris GL, Black HR, Cushman WC, Green LA, Izzo JL, Jr., Jones DW, Materson BJ, Oparil S, Wright JT, Jr. and Roccella EJ**. The Seventh Report of the Joint National Committee on Prevention, Detection, Evaluation, and Treatment of High Blood Pressure: The JNC 7 Report. *JAMA* 289: 2560-2571, 2003.

4. **De Jong JC, Willems PH, Mooren FJ, van den Heuvel LP, Knoers NV and Bindels RJ**. The structural unit of the thiazide-sensitive NaCl cotransporter is a homodimer. *J Biol Chem* 278: 24302-24307, 2003.
5. **Dumont J N**. Oogenesis in *Xenopus laevis* (Daudin). Stages of oocyte development in laboratory maintained animals. *J Morph* 136: 153-180, 1970.
6. **Gamba G, Miyanoshita A, Lombardi M, Lytton J, Lee WS, Hediger MA and Hebert SC**. Molecular cloning, primary structure and characterization of two members of the mammalian electroneutral sodium-(potassium)-chloride cotransporter family expressed in kidney. *J Biol Chem* 269: 17713-17722, 1994.
7. **Gamba G, Saltzberg S N, Lombardi M, Miyanoshita A, Lytton J, Hediger M A, Brenner B M and Hebert S C**. Primary structure and functional expression of a cDNA encoding the thiazide-sensitive, electroneutral sodium-chloride cotransporter. *Proc Natl Acad Sci USA* 90: 2749-2753, 1993.
8. **Gamba G**. Molecular physiology and pathophysiology of the electroneutral cation-chloride cotransporters. *Physiol Rev* 85: 423-493, 2005.
9. **Gao X, Lu F, Zhou L, Dang S, Sun L, Li X, Wang J and Shi Y**. Structure and mechanism of an amino acid antiporter. *Science* 324: 1565-1568, 2009.
10. **Gray TM and Matthews BW**. Intrahelical hydrogen bonding of serine, threonine and cysteine residues within alpha-helices and its relevance to membrane-bound proteins. *J Mol Biol* 175: 75-81, 1984.
11. **Hediger MA, Romero MF, Peng JB, Rolfs A, Takanaga H and Bruford EA**. The ABCs of solute carriers: physiological, pathological and therapeutic implications of human membrane transport proteinsIntroduction. *Pflugers Arch* 447: 465-468, 2004.

12. **Hoover RS, Poch E, Monroy A, Vazquez N, Nishio T, Gamba G and Hebert SC**. N-Glycosylation at Two Sites Critically Alters Thiazide Binding and Activity of the Rat Thiazide-sensitive Na(+):Cl(-) Cotransporter. *J Am Soc Nephrol* 14: 271-282, 2003.
13. **Isenring P, Jacoby S C, Chang J and Forbush III B**. Mutagenic mapping of the Na-K-Cl cotransporter for domains involved in ion transport and bumetanide binding. *J Gen Physiol* 112: 549-558, 1998.
14. **Krishnamurthy H, Piscitelli CL and Gouaux E**. Unlocking the molecular secrets of sodium-coupled transporters. *Nature* 459: 347-355, 2009.
15. **Monroy A, Plata C, Hebert SC and Gamba G**. Characterization of the thiazide-sensitive Na(+)-Cl(-) cotransporter: a new model for ions and diuretics interaction. *Am J Physiol Renal Physiol* 279: F161-F169, 2000.
16. **Moreno E, San Cristobal P, Rivera M, Vazquez N, Bobadilla NA and Gamba G**. Affinity defining domains in the Na-Cl cotransporter: different location for Cl- and thiazide binding. *J Biol Chem* 281: 17266-17275, 2006.
17. **Novello F C and Sprague J M**. Benzothiadiazine dioxides as novel diuretics. *J Am Chem Soc* 79: 2028-2029, 1957.
18. **Sabath E, Meade P, Berkman J, De Los HP, Moreno E, Bobadilla NA, Vazquez N, Ellison DH and Gamba G**. Pathophysiology of Functional Mutations of the Thiazide-sensitive Na-Cl Cotransporter in Gitelman Disease. *Am J Physiol Renal Physiol* 287: F195-F203, 2004.
19. **San Cristobal P, De Los HP, Ponce-Coria J, Moreno E and Gamba G**. WNK Kinases, Renal Ion Transport and Hypertension. *Am J Nephrol* 28: 860-870, 2008.
20. **Shaffer PL, Goehring A, Shankaranarayanan A and Gouaux E**. Structure and mechanism of a Na+-independent amino acid transporter. *Science* 325: 1010-1014, 2009.

21. **Tovar-Palacio C, Bobadilla NA, Cortes P, Plata C, De Los HP, Vazquez N and Gamba G**. Ion and Diuretic Specificity of Chimeric Proteins Between Apical Na+:K+:2Cl- and Na+:Cl- Cotransporters. *Am J Physiol Renal Physiol* 287: F570-F577, 2004.

22. **Vazquez N, Monroy A, Dorantes E, Munoz-Clares RA and Gamba G**. Functional differences between flounder and rat thiazide-sensitive Na- Cl cotransporter. *Am J Physiol Renal Physiol* 282: F599-F607, 2002.

23. **Yamashita A, Singh SK, Kawate T, Jin Y and Gouaux E**. Crystal structure of a bacterial homologue of Na+/Cl--dependent neurotransmitter transporters. *Nature* 437: 215-223, 2005.

Figure legends

Figure 1. General topology and alignment analysis of TM regions 8 to 12 in mammalian and flounder NCCs. The proposed topology for NCC includes a central hydrophobic domain made up of 12 putative transmembrane segments divided into two fragments by a large extracellular glycosylated loop between segments 7 and 8. The central hydrophobic domain is flanked by intracellular short and long amino and carboxyl terminal domains. Alignment analysis of TM segments 8 to 12 is shown. Amino acid residues in boxes are those less conserved between flounder and all mammalian sequences and were thus the residues chosen for study.

Figure 2. Mutant constructs for TM9, TM11, and TM12 are functional. The percentage of rNCC activity in wild-type and mutant NCCs. The thiazide-sensitive $^{22}Na^{+}$ uptake in wild-type NCC was set as 100%, and the values observed in mutant clones were normalized accordingly. At least five different 10 oocyte experiments were done. Normalization of data was done for each experiment before comparing the groups. The data shown represent the mean ± S.E.M. of five different experiments. *$p<0.05$ vs. wild-type NCC.

Figure 3. The effect of TM mutations on rNCC affinity for metolazone. Metolazone dose-response analysis was assessed in five different experiments, in all of which the five different clones were tested simultaneously, using the same uptake solutions and metolazone dilutions. A) A compilation of the dose-response curves from the five experiments is shown. Wild-type rNCC (blue), wild-type flNCC (red), TM9 mutant (orange), TM12 mutant (pink), and TM11 mutant (green). Data were fit to the Hill equation and in all cases Hill coefficients close to unity were obtained. All group data are shown as mean ± S.E.M of percentage of activity. The coefficient of determination (R^2) was between 0.95 and 0.99 for the fits shown. B) Metolazone IC_{50} for rNCC

and mutants calculated from the nonlinear regression fit of uptake data to the Hill equation. Data are shown as mean IC_{50} ± S.E.M. of five different experiments. *p<0.05 vs. rNCC

Figure 4. The effect of individual mutations in the rNCC TM11 segment on the affinity for metolazone. Methods are similar to those explained in Figure 3, and five different experiments were performed. The bars represent mean IC_{50} ± S.E.M for each tested clone, as stated. For each experiment all Hill slopes were ~1 and coefficients of determination (R^2) were between 0.92 and 0.99. *p<0.05 vs. rNCC.

Figure 5. The effect of TM mutations in flNCC on the affinity for metolazone. Metolazone dose-response analysis was assessed as explained in Figure 3. Similar observations were done in three different experiments. A) A representative experiment is shown. Dose-response curves are shown for wild-type flNCC (squares) and C576S-flNCC (circles). The coefficient of determination (R^2) was 0.96 and 0.98, respectively. B) Metolazone IC_{50} for flNCC and C576S mutant was calculated from the nonlinear regression fit of uptake data to the Hill equation. Data are shown as mean IC_{50} ± S.E.M. of three different experiments. *p<0.05 vs. flNCC.

Figure 6. TM11 mutant rNCC and the single mutant S575C-rNCC exhibited higher activity than wild-type NCC or I574C-rNCC. Oocytes were injected with the same amount of cRNA of each clone, as explained in the text. A) Three days later the $^{22}Na^+$ uptake was assessed in the absence (open bars) or presence (closed bars) of metolazone. Data presented are mean ± S.E.M. of the uptake observed for each oocytes. Similar observations were done in at least five experiments. *p<0.05 vs. control wild-type rNCC. B) Proteins were extracted for a western blot analysis using

anti-FLAG or anti-actin antibody. A representative western blot is shown in B. C) Densitometric analysis of bands observed in the western blot.

Figure 7. Functional expression and metolazone affinity of mutant rNCCs S575C, S575A, S575D, and S575K. Oocytes were injected with cRNA from each mutant clone. A) Three days later, the $^{22}Na^{+}$ uptake was assessed in the absence (open bars) or presence (closed bars) of 100 μM metolazone. Data are mean ± S.E.M. B) Metolazone IC_{50} values for rNCC and mutants were calculated from the nonlinear regression fit of uptake data to the Hill equation. Data are shown as mean IC_{50} ± S.E.M. of 3 different experiments. *$p<0.05$ vs. rNCC.

Figure 8. Electrophoretic behavior of rNCC and S575C-rNCC in the absence or presence of a reducing agent. Protein extracts from oocytes injected with water, rNCC cRNA, or rNCC-S575C cRNA were diluted for standard SDS-PAGE in Laemmli buffer without reducing agent (A), or containing either 0.5% (B), 2.5% (C) or 5% (D) β-mercaptoethanol. In the absence of reducing agent (A), bands of expected size for monomeric and dimeric forms of the cotransporter were observed, and in both cases, a diffused signal of slightly higher molecular weight was detected which probably corresponds to glycosylated forms of the protein. This was seen for the wild-type and mutant form of rNCC. In the presence of reducing agent, the bands corresponding to the dimeric form of the cotransporter disappeared even at the lowest concentration of reducing agent used. At this concentration, we were able to observe a slight signal corresponding to the dimers, but no difference in intensity was observed between the wild type and the mutant.

554 Table 1. Ion transport affinities in rNCC, flNCC and mutant clones

555

	rNCC	TM9	TM11	TM12	flNCC
Na^+ Km (mM)	6.95 ± 1.8	9.2 ± 1.5	7.7 ± 1.3	8.6 ± 1.3	31 ± 4.3
Cl^- Km (mM)	5.25 ± 2.0	4.1 ± 1.3	4.8 ± 1.0	3.3 ± 1.2	14 ± 1.3

559

560

561

562

563

564

Figure 1

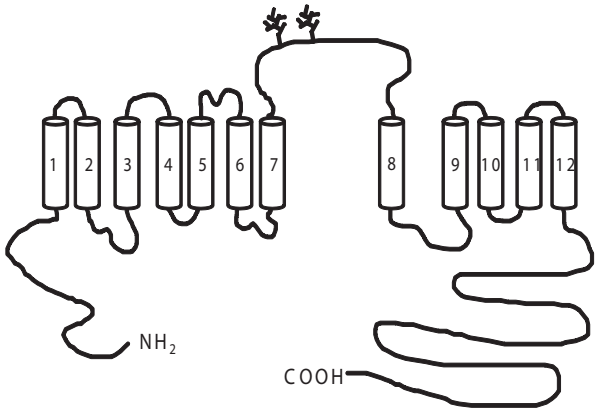

TM8

```
Rat       FAPLITAGIFGATLSSALAC
Mouse     FAPLITAGIFGATLSSALAC
Human     FAPLITAGIFGATLSSALAC
Rabbit    FAPLITAGIFGATLSSALAC
Flounder  FAPLISAGIFGATLSSALAC
```

TM9

```
Rat       LAYAIAVAFIIIAELNTIAP
Mouse     LAYAIAVAFIIIAELNTIAP
Human     LAYAIAVAFIIIAELNTIAP
Rabbit    LAYAIAVAFIIIAELNTIAP
Flounder  LTYVIAVCFVLIAELNTIAP
```

TM10

```
Rat       IISNFFLCSYALINFSCFHA
Mouse     IISNFFLCSYALINFSCFHA
Human     IISNFFLCSYALINFSCFHA
Rabbit    IISNFFLCSYALINFSCFHA
Flounder  IISNFFLCSYALINFSCFHA
```

TM11

```
Rat       KWAALFGAVISVVIMFLLTW
Mouse     KWAALFGAVISVVIMFLLTW
Human     KWAALFGAIISVVIMFLLTW
Rabbit    KWSALFGAVVSVVIMFLLTW
Flounder  KWLSLLGAVCCVVIMFLLTW
```

TM12

```
Rat       WAALIAIGVVLFLLLYVIYK
Mouse     WAALIAIGVVLFLLLYVIYK
Human     WAALIAIGVVLFLLLYVIYK
Rabbit    WAALIAIGVILFLLLYVIYK
Flounder  WAALIAFGVVFFLLGYTLYK
```

Figure 2

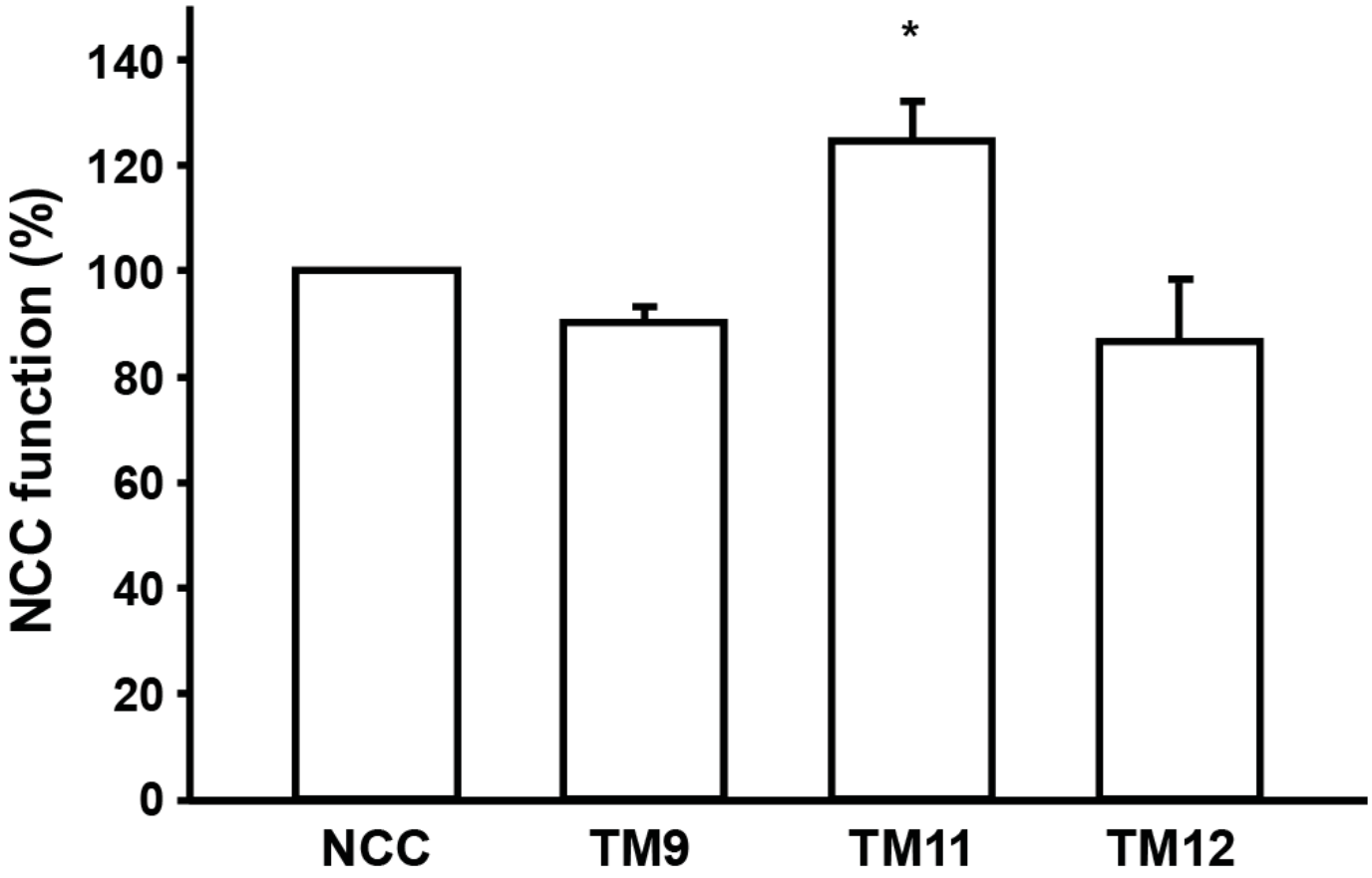

Figure 3

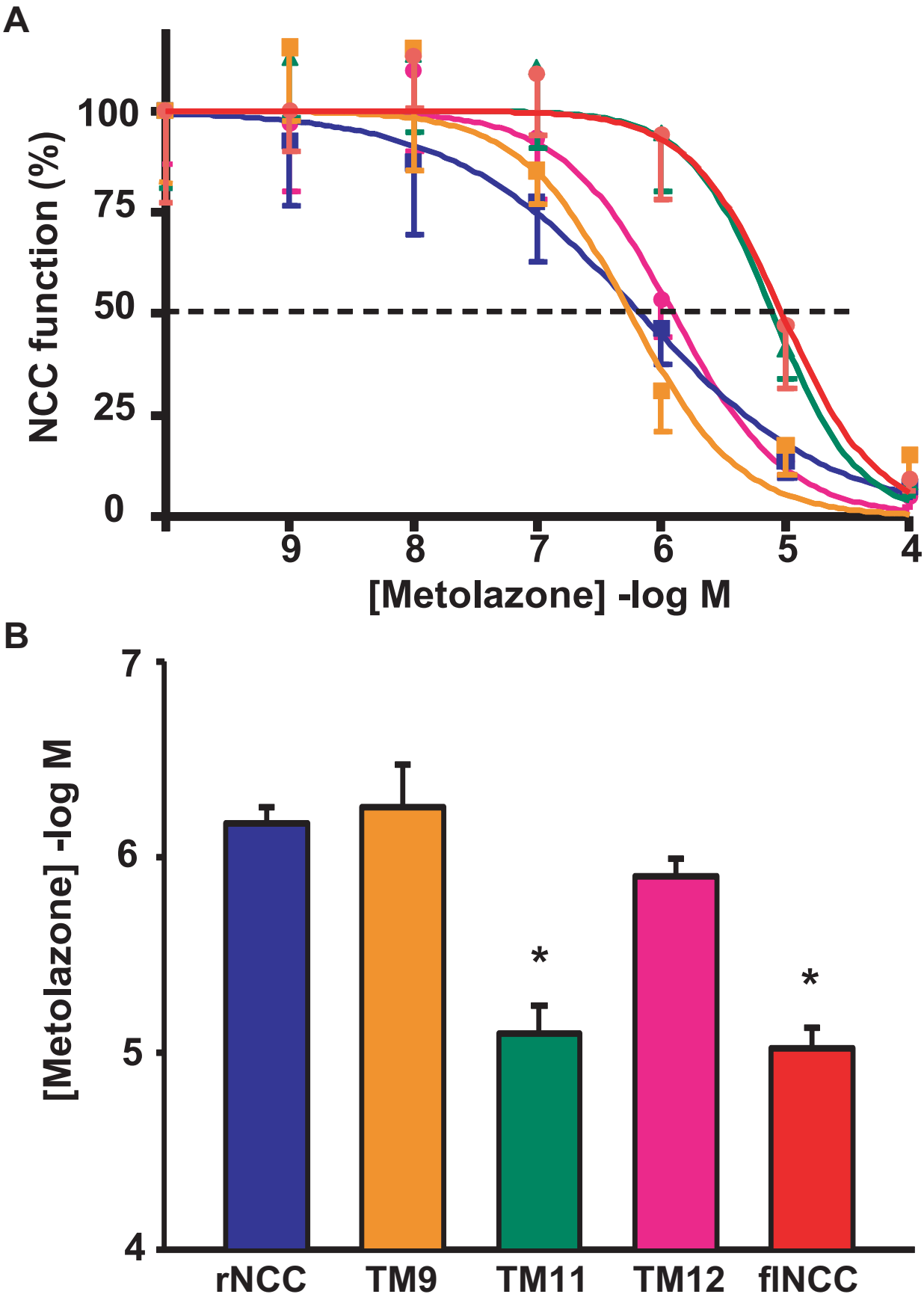
A
NCC function (%)
100
75
50
25
0
9
8
7
6
5
4
[Metolazone] -log M
B
[Metolazone] -log M
7
6
5
4
*
*
rNCC
TM9
TM11
TM12
fINCC

Figure 4

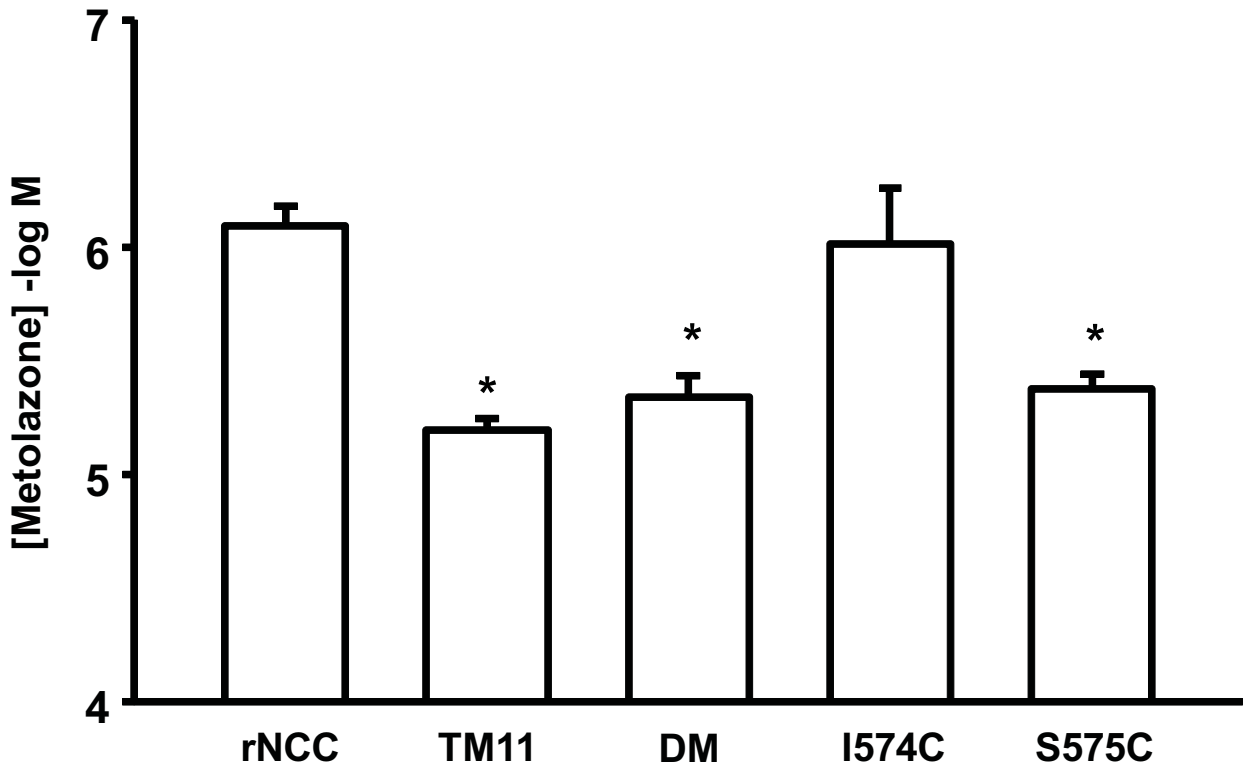

Figure 5

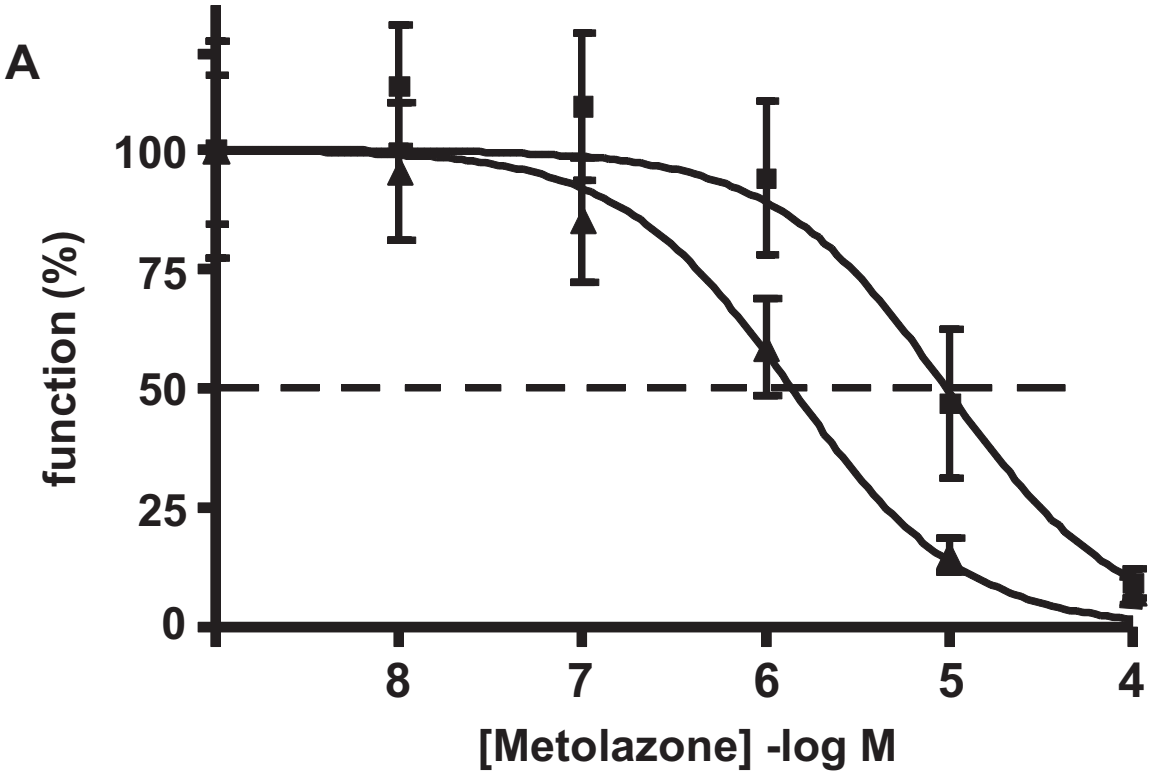
A
100
75
50
25
0
function (%)
8
7
6
5
4
[Metolazone] -log M

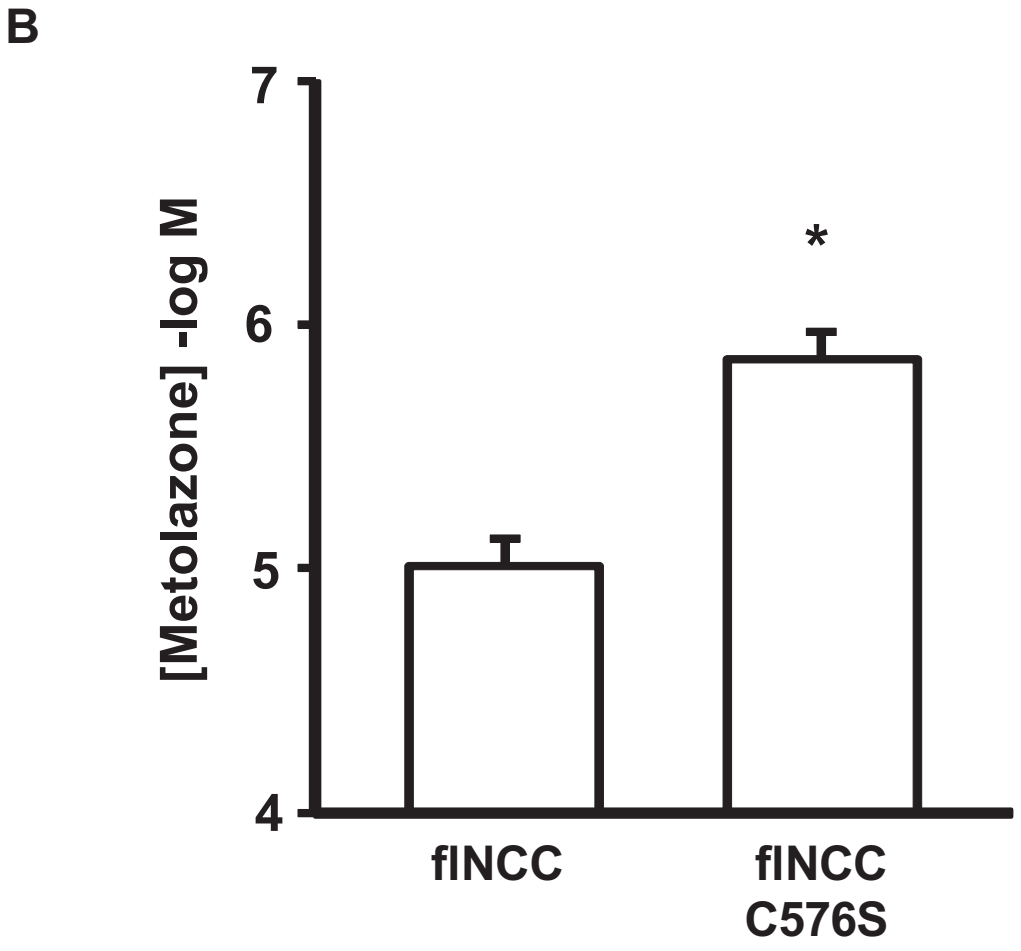
B
7
6
5
4
[Metolazone] -log M
*
fINCC
fINCC
C576S

Figure 6

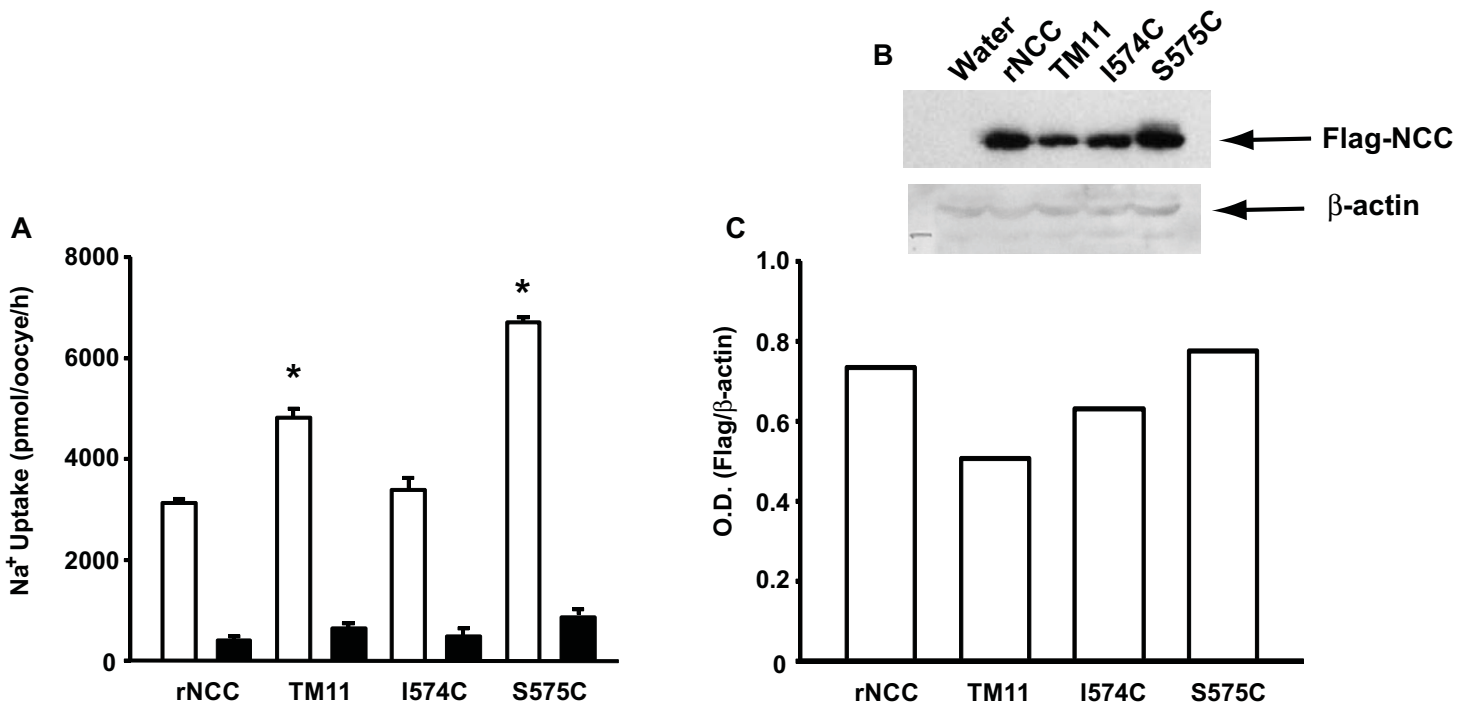
A
Na+ Uptake (pmol/oocye/h)
8000
6000
4000
2000
0
*
*
rNCC
TM11
I574C
S575C
B
Water
rNCC
TM11
I574C
S575C
Flag-NCC
β-actin
C
O.D. (Flag/β-actin)
1.0
0.8
0.6
0.4
0.2
0
rNCC
TM11
I574C
S575C

Figure 7

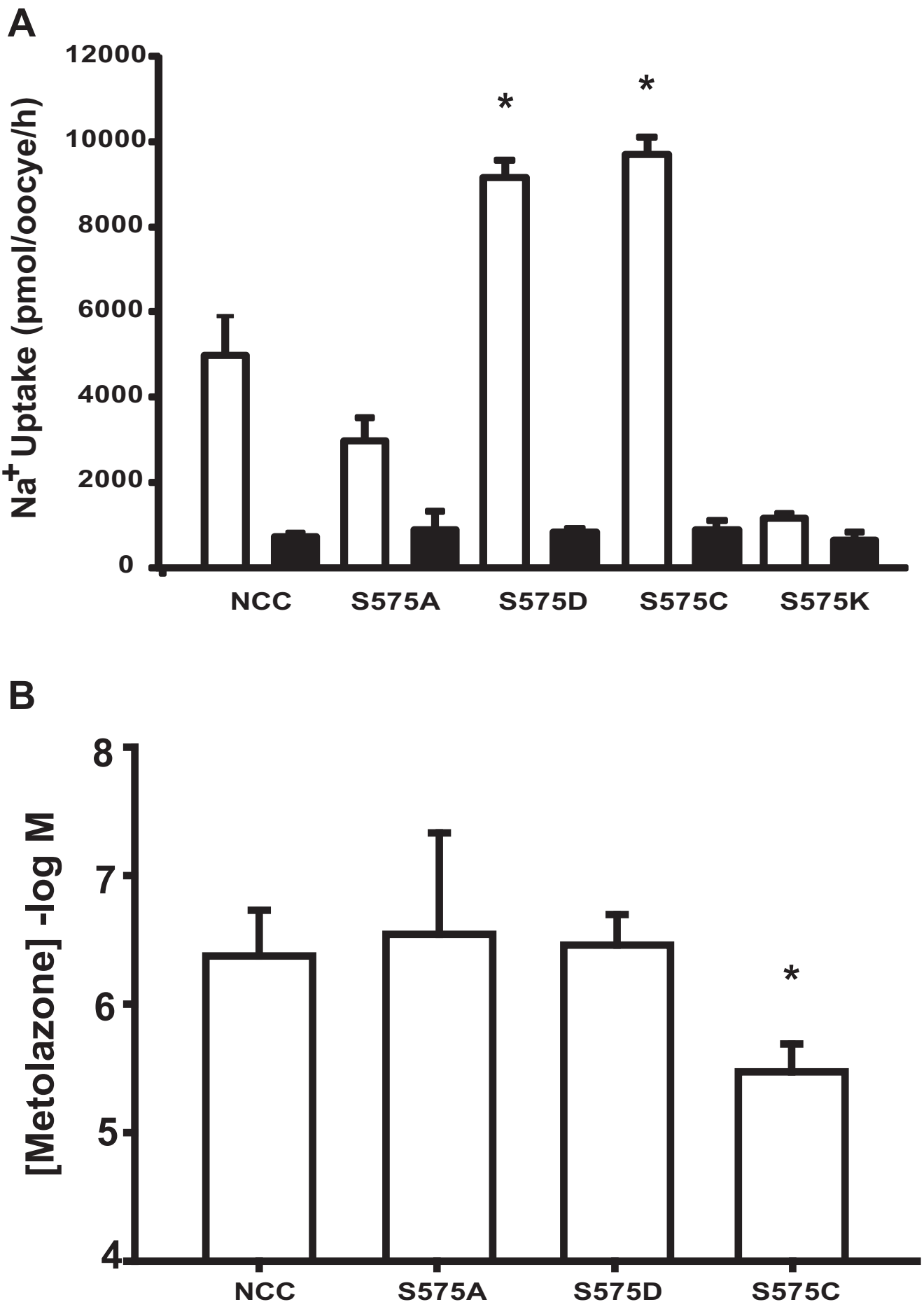
A
12000
10000
8000
6000
4000
2000
0
Na+ Uptake (pmol/oocye/h)
*
*
NCC
S575A
S575D
S575C
S575K
B
8
7
6
5
4
[Metolazone] -log M
*
NCC
S575A
S575D
S575C

Figure 8

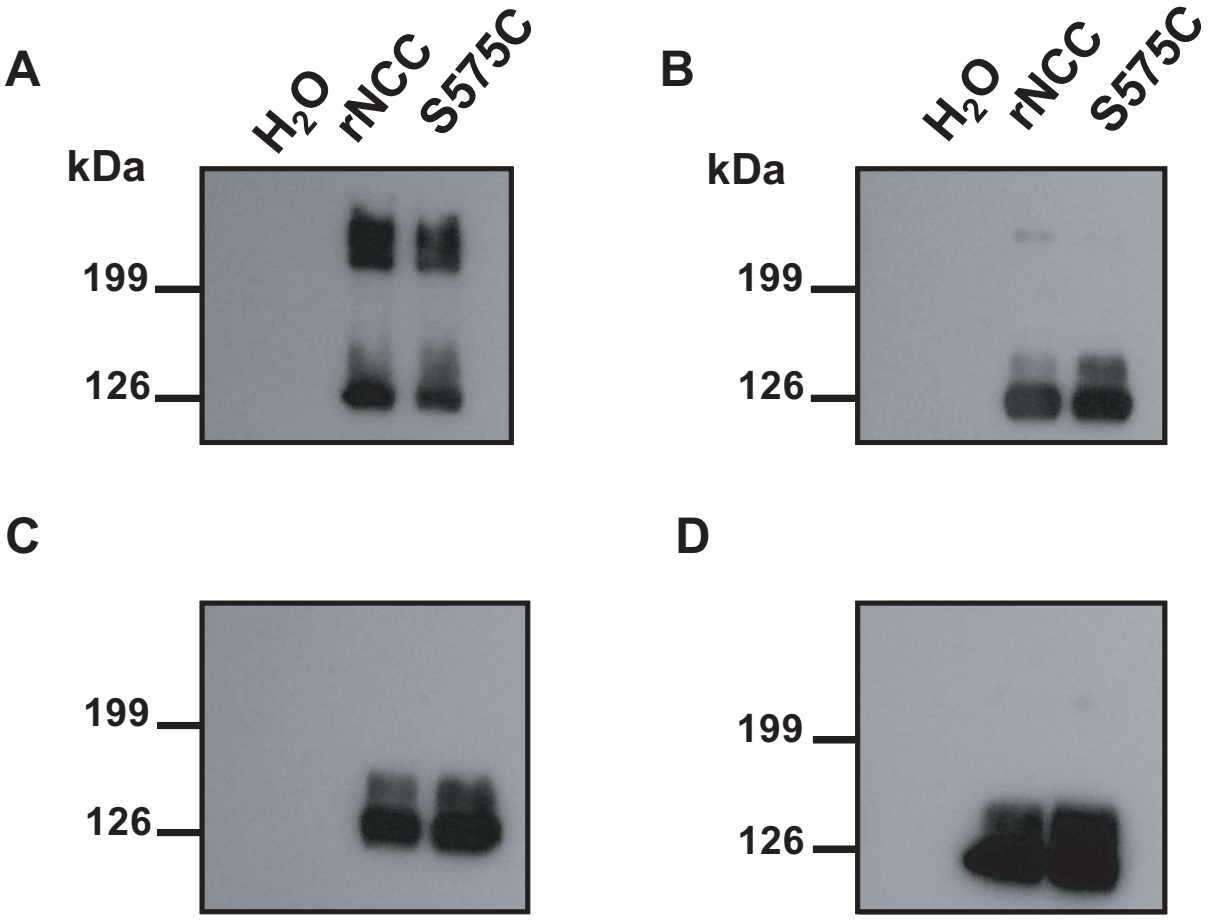
A
H2O
rNCC
S575C
kDa
199
126
B
H2O
rNCC
S575C
kDa
199
126
C
199
126
D
199
126